Youssef Mahjoub, Amel Soualmia, Azeddine Kourta
Bridge Piers Configuration and Flood Management: A Numerical Analysis of Medjerda River DynamicsInternational Journal Water Sciences and Environment Technologies
Vol. (ix), Issue. 3, November 2024, pp. 37- 45
ISSN Online: 1737-9350; ISSN Print: 1737-6688, Open Access
www.jiste.org
Scientific Press International Limited
Received: March 2024 / Revised: April 2024 / Accepted: July 2024 / Published: November 2024

Bridge Piers Configuration and Flood Management: A Numerical Analysis of Medjerda River Dynamics

Youssef Mahjoub[1], Amel Soualmia[2], Azeddine Kourta[2]

1 Department of Rural Engineering, Water and Forestry, National Agricultural Institute of Tunis, Carthage University, Tunis, Tunisia.

2 INSA-CVL, PRISME, University of Orleans, Orleans, France.

Abstract

Designing hydraulic structures such as bridges, dams, and irrigation canals necessitates a thorough understanding of associated hydraulic flow phenomena. Flow characteristics differ at various stages: before, during, and after passage through these structures. This study conducted a numerical analysis focusing on different geometries of obstacles in open channels to better understand the hydraulic jump following structure-fluid interaction.

Two geometric configurations of bridge piers (initially two piers, then three) were simulated using the finite volume method in ANSYS-FLUENT. The objective was to assess how geometry affects flow characteristics under identical hydrodynamic conditions. Non-slip walls were assumed for all fluid-solid interaction surfaces, including piles, bed, and sidewalls. The study aimed to highlight pressures, velocity fields, and hydraulic properties derived from the modeling.

A comparative analysis of the numerical results for the two configurations evaluated the flow characteristics. The simulations provided a comprehensive understanding of water behavior, detailing the variability of the velocity field and the impact of water pressure on obstacles. This research offers valuable insights into developing effective river management strategies, improving our ability to mitigate risks, and enhancing environmental safety amid changing conditions.

Key Words*:* Water erosion, Watershed, Modelling, RUSLE, GIS, Anti-erosion developments.

Configuration des piliers de pont et gestion des crues : analyse numérique de la dynamique de la rivière Medjerda

Résumé

La conception d'ouvrages hydrauliques tels que des ponts, des barrages et des canaux d'irrigation nécessite une compréhension approfondie des phénomènes d'écoulement hydraulique associés. Les caractéristiques d'écoulement diffèrent à différentes étapes : avant, pendant et après le passage dans ces ouvrages. Cette étude a mené une analyse numérique axée sur différentes géométries d'obstacles dans des canaux ouverts pour mieux comprendre le ressaut hydraulique suite à l'interaction structure-fluide.

Deux configurations géométriques de piles de pont (initialement deux piles, puis trois) ont été simulées en utilisant la méthode des volumes finis dans ANSYS-FLUENT. L'objectif était d'évaluer comment la géométrie affecte les caractéristiques d'écoulement dans des conditions hydrodynamiques identiques. Des parois antidérapantes ont été supposées pour toutes les surfaces d'interaction fluide-solide, y compris les pieux, le lit et les parois latérales. L'étude visait à mettre en évidence les pressions, les champs de vitesse et les propriétés hydrauliques dérivées de la modélisation.

Une analyse comparative des résultats numériques pour les deux configurations a évalué les caractéristiques d'écoulement. Les simulations ont fourni une compréhension globale du comportement de l'eau, détaillant la variabilité du champ de vitesse et l'impact de la pression de l'eau sur les obstacles. Cette recherche offre des informations précieuses sur l'élaboration de stratégies efficaces de gestion des rivières, l'amélioration de notre capacité à atténuer les risques et le renforcement de la sécurité environnementale dans des conditions changeantes.

Mots clés : Érosion hydrique, Bassin Versant, Modélisation, RUSLE, SIG, Aménagements antiérosifs.

[1] Corresponding author: amel.inat@hotmail.fr

1. INTRODUCTION

Throughout history, from ancient times to the present day, humans have maintained a profound connection with water, acknowledging it as a fundamental source of life for all living beings.

To manage effectively its use, humanity has consistently resorted to constructing civil engineering infrastructures to harness, cross, or utilize water from various watercourses [1].

This has entailed the development of dams, canals, aqueducts, and other structures that influence the natural flow of water and its hydraulic characteristics. Throughout history, civil and water resource engineers have played a critical role in advancing our understanding of water systems and designing efficient infrastructure for water management [2, 3].

Throughout history, bridges have served as vital connectors, their design evolving alongside advancements in geometry. From the simple structures of ancient civilizations to the remarkable geometric precision [4], the role of geometry in bridge design continued to expand. In medieval Europe, the creation of detailed stone bridge designs underscored the increasing focus on structural integrity [3, 4]. This evolution in bridge design became particularly crucial for managing flood risks, with the configuration of bridge piers playing a critical role in regions prone to flooding, like the Medjerda River basin. The Renaissance further solidified this synergy between geometry, bridge construction, and water management, influencing modern bridge designs [5].

While a substantial body of literature exists on flow-cylinder interaction, a knowledge gap persists concerning the hydrodynamic problem perspective [6]. Prior studies have primarily investigated the phenomenon from a kinematic standpoint, aiming to resolve the coherent flow structures (e.g., horseshoe vortices, down flow) generated around the cylinder by using point measurements and experimental observations [7]. However, these approaches often lack in-depth analysis of the underlying hydrodynamic forces and mechanisms governing the interaction [8, 9]. Consequently, the following research questions remain unaddressed:

- How does the number of piers affect the velocity distribution and control the backflow regions near to the structure ?
- How does bed shear stress change depend on the number of piers?
- How does the number of bridge piers control the spatial distribution of the shear stress on the cylinders' surface and the bottom around them?

The primary object of this study is to find answers to these questions for this particular case and open new perspectives for water-obstacle comportment studies. The numerical model has enabled us to study the flow and scour processes, particularly concerning the issues referred to in the preceding paragraph.

2. METHODOLOGY

2.1. Domaine assumption

To enhance the relevance and value of our study, we chose to employ a real-scale case. The configuration of this type of bridge is frequently used in the Medjerda River in Tunisia and has been prevalent since the early 1980s to the present [5].

A 250 m long by 20 m high and 80 m rectangular canal was used for the simulation. Figure 1 depicts the placement of the bridge, situated 50 meters from the entry of the channel.

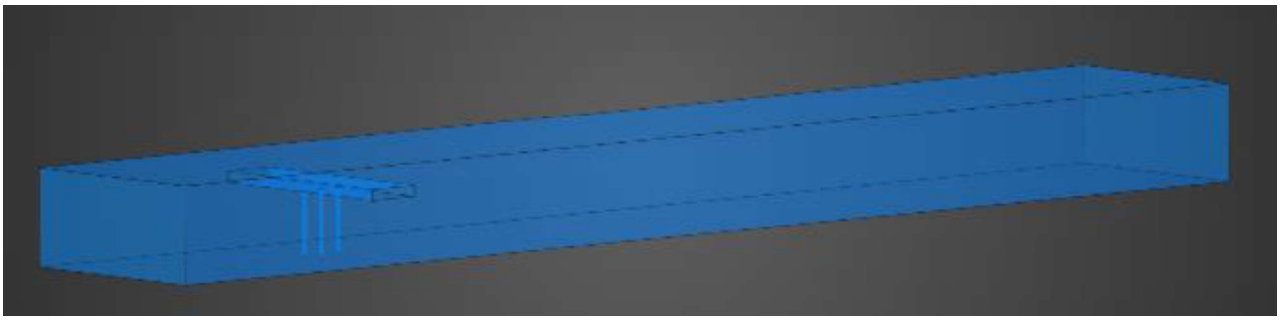

Fig. 1 - 3D Numerical Model of Bridge Pier Configuration within a channel

2.2 Governing equations

In this section, a description of the computational model used throughout the present work provided the physical principles of conservation between pressure and velocity are described by the Navier-Stokes equations. These non-linear partial differential equations characterize the monophasic turbulent flow in an open channel at each point in the fluid [10, 11, 12]. The numerical solves the incompressible RANS equation:

$$\rho \frac{\partial \overline{u_i}}{\partial t} + \rho \overline{u_j} \frac{\partial \overline{u_i}}{\partial x_j} = -\frac{\partial \overline{p}}{\partial x_i} + \frac{\partial}{\partial x_j}\left(\overline{\tau_{ij}} + \overline{\tau_{ij}'}\right) + \rho g_i \quad (1)$$

Where:

ρ: Fluid density
U : Longitudinal velocity vector
u_i: The component of the velocity vector in the I direction
t : Time
g_i: The component of the gravity vector in the I direction
μ: Viscosity
p: Static pressure
x_i: x component in the I direction
τ_{ij}: Tensor viscous stresses
$\overline{\tau_{ij}'}$: Reynolds stress tensor

The equation presented is the Navier-Stokes equation for fluid motion in its incompressible form. This equation describes the momentum balance in a fluid flow, accounting for various forces acting on a fluid particle [10, 13]. The first term represents the rate of change of momentum per unit volume of the fluid. The second term describes the convective transport of momentum, indicating how the fluid's momentum changes as it moves through space [14]. The third term represents the pressure gradient force per unit volume, highlighting the influence of pressure differences within the fluid [12, 15]. The fourth term accounts for the viscous stresses and Reynolds stresses in the fluid, incorporating both the internal friction due to fluid viscosity and the turbulent fluctuations [15]. Finally, the last term represents the gravitational force per unit volume, reflecting the effect of gravity on the fluid.

In summary, the Navier-Stokes equation balances the inertial forces, pressure forces, viscous forces, and gravitational forces acting on a fluid element.

The introduction of the Reynolds stress tensor leads to nonlinear terms in the equation, hence the need for a closure model. This model helps to represent the complex interactions between different components of turbulence and to estimate their overall effect on the mean flow. The Boussinesq hypothesis aids in resolving the closure issue by introducing Reynolds stresses, which make the equation system more adaptable and describe how turbulence affects the evolution of the mean flow [14, 15].

$$-(\rho \overline{u_i u_j}) = \mu_t\left(\frac{\partial u_i}{\partial x_j} + \frac{\partial u_j}{\partial x_i}\right) + \frac{2}{3}(\rho k)\delta_{ij} \quad (2)$$

There are many closure models available, but we have chosen to use the RSM closure model for our case. This decision is based on its extensive use in similar situations and its proven effectiveness in the literature [11].

To resume, before the numerical methods application, the Navier–Stokes equations are time-averaged (or ensemble-averaged in flows with time-dependent boundary conditions). Extra terms appear in the time-averaged (or Reynolds-averaged) flow equations due to the interactions between various turbulent fluctuations. This extra term is modeled with classical turbulence models. The K-omega was chosen after numerical validation and bibliographic research. For the ANSYS Fluent setup, we used the "Double Precision" option in 2D, incorporating gravitational acceleration, and the standard k-omega model.

2.2.2 Biphasic turbulent flow Reynolds equations

The Eulerian formulation of the Navier-Stokes incompressible equation for a non-miscible biphasic flow requires a numerical solution to determine the position of the interface between different fluid streams [8, 10, 11]. The interface capture method involves identifying the free surface within a fixed mesh in the domain containing the free interface. This approach differs from methods that track the deformations of the mesh's free surface [12]. The main advantage

of these capture techniques is their ability to model flows with interface reconnections [11]. In this context, the technical method used to address the topological evolution of a biphasic region is the volume of fluid (VOF) approach, initially proposed by Hirt and Nichols. The continuity equation for phase q is derived from the following relations.

$$div(c_q \rho_q v_q) = \sum_{p=1}^{2} m_{pq} \quad (3)$$

Where m_{pq} represents the mass transfer of the pth phase at a qth phase: $m_{12} = m_{21}$ and $m_{pp} = 0$. m_{pq} is the volume mass of the phase q and υ_q is the volume. The equation for the conservation of momentum during phase q is given by the following relation:

$$div(c_q \rho_q \vec{v}_q \vec{v}_q) = -c_q \overrightarrow{grad} p + div\overline{\tau_q} + \sum_{p=1}^{2}(\overrightarrow{R_{pq}} + m_{pq} + \overrightarrow{v_{pq}}) + c_q \rho_q (\overrightarrow{F_q} + \overrightarrow{F_{VMq}}) \quad (4)$$

Where :

$\overline{\tau}$: Shear stress of q^{th} phase (pa);
$\overrightarrow{F_q}$: Exterior force of volume (N/kg);
$\overrightarrow{F_{VMq}}$: Added mass force (N/kg);
$\overrightarrow{R_{pq}}$: Interaction force at the interface;
c_q: Void fraction of phase q;

2.3 Numerical Algorithm

The generation of mesh geometry by a pre-processor marks the transition from the physical realm to the numerical domain. Once created, this mesh is imported into computational code to iteratively solve equations and determine the parameters at each mesh node. The governing equations and turbulence model were resolved using a segregated solution approach, while the control volume technique was used to discretize the governing equations.

The SIMPLE (Semi-Implicit Method for Pressure-linked Linked Equations) method was utilized to simulate the velocity-pressure coupling within a multiphase model (VOF). To model the convective and diffusive terms, a second-order upwind method was applied.

The rise of relative residuals in each governing equation was tracked, with a convergence criterion of 0.001% to confirm the convergence of the numerical calculation. Relaxation coefficients for velocity, pressure, and other parameters were used to ensure the stability of the iterative process. The effects of friction near the wall were considered using the Standard Wall-Functions. Three different mesh distributions were analyzed to ensure grid-independent results, a crucial step for simulation accuracy and reliability. Using Fluent Mesh, we tested coarse, intermediate, and fine distributions. The coarse mesh, with fewer cells, allowed faster but less precise calculations. The intermediate mesh balanced resolution and computational time, capturing better gradients without excessive load. The fine mesh, with the highest resolution, provided maximum accuracy at the cost of longer computation. Comparing results from these meshes confirmed solution convergence, ensuring differences became negligible with finer meshes. This validated the independence of results from the mesh used, enabling the selection of the optimal balance of precision and efficiency.

3. RESULTS AND DISCUSSIONS

In previous sections, we introduced our study's framework and extensively developed our prototype using CFD simulations. This section unveils primary outcomes from geometric and numerical simulations, highlighting the imperative for a more in-depth investigation of the problem.

3.1 Mesh geometry generating

The mesh geometry was generated with specific settings to ensure accuracy and efficiency. Adaptive sizing was not utilized, with the growth rate set to the default value of 1.2 and a maximum element size of 4 m. Mesh defeaturing was enabled, using a defeature size of 1 cm to simplify small features. Curvature capture was activated, with the minimum curvature size set to 2.2 e^{-002} m and the curvature normal angle set to 18°. The bounding box diagonal measured 253.82 m, the average surface area was 2420.6 m^2, and the minimum edge length was 2.0 cm.

In terms of quality, no automatic inflation was applied. Instead, a smooth transition inflation option was selected, with a transition ratio of 0.272, a maximum of 5 layers, and a growth rate of 1.2. The pre-inflation algorithm was used to enhance the mesh quality near boundaries. The final mesh consisted of 65,748 nodes and 346,389 elements, ensuring a detailed and accurate representation of the geometry.

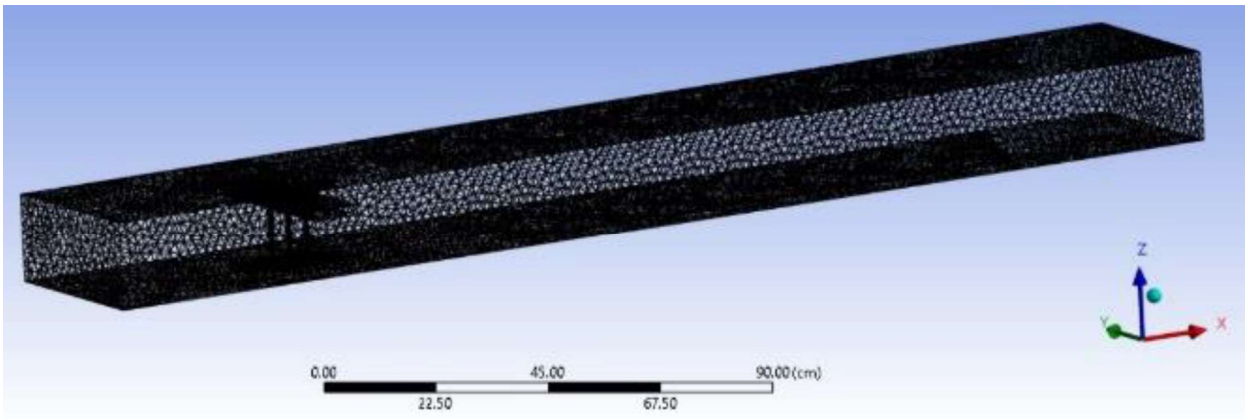

Fig. 2 - Grid configuration and mesh outcome

The mesh geometry was generated to accurately represent the riverbed and the configurations of the bridge piers. For the double piers configuration, two cylindrical piers were positioned symmetrically in the river. The mesh included finer elements around the piers to capture detailed flow patterns and turbulence. In contrast, the triple piers configuration involved an additional cylindrical pier, increasing the complexity of the mesh. This required further refinement to accurately simulate the increased turbulence and interactions between the piers, particularly in the regions where flow separation and recirculation occur.
Near the scours, where there is a significant velocity gradient, the mesh is uniformly very fine. The grid distribution affects both the amount of time required for calculation as well as how many iterations must occur for a given solution to converge.

3.2 Discussion of the velocity field

In the double piers configuration (figure 3. a), the velocity field showed moderate deviations around the piers. The flow maintained a relatively smooth pattern, with slight accelerations were observed in the recirculation zones behind the piers. In contrast, the water surface in the second configuration (figure 3. b) was significantly more disturbed compared to the two-pier setup.
Visible waves and elevated water levels are observed around each pier, particularly in the areas between the piers, indicating heightened turbulence and flow disruption.

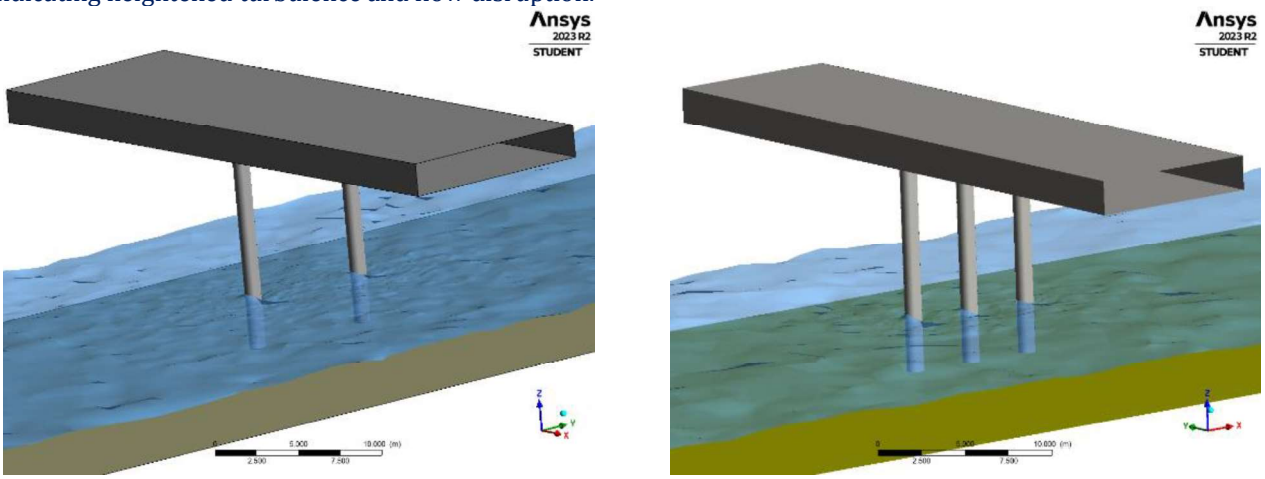

a) Two piers configuration bridge b) Three piers configuration bridge

Fig. 3 - Water Surface Behavior around Bridge Pier Configuration

The Navier-Stokes equations, which govern fluid flow, explain these observations through the balance of inertial and viscous forces. The presence of the piers disrupts the flow, causing local accelerations (due to reduced cross-sectional area) and decelerations (due to flow separation).
The double piers configuration (in Figure 4. a) displayed recirculation zones behind the piers, with water velocities generally lower in these areas due to the flow separation. The velocities in these recirculation zones were approximately 20% lower than the free stream velocity, resulting in smoother flow patterns and so with lower turbulence. The impact on the overall flow dynamics was relatively moderate, allowing the river to maintain its general flow direction with minimal disturbance.

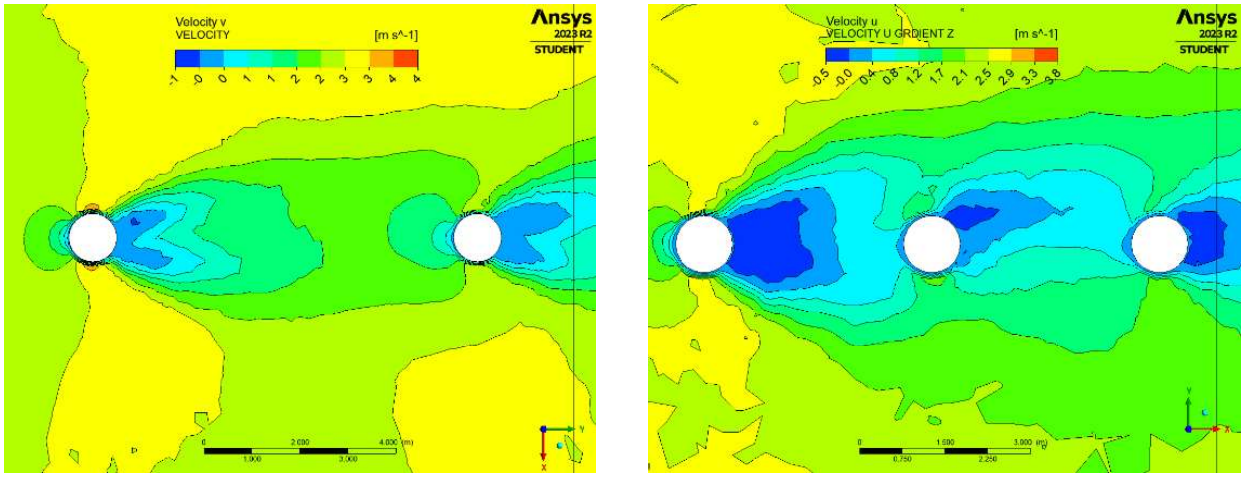

a) Two piers configuration bridge b) Three piers configuration bridge

Fig. 4 - Contour of X-direction velocities differences between the two piers Two piers configuration bridge (a), and the three piers configuration bridge (b)

In contrast, the triple piers configuration (in Figure 4. b) exhibited significant deflections and higher turbulence in the velocity field. The flow became uneven, with pronounced accelerations and decelerations around the piers. The continuity equation (conservation of mass) requires that the same volume of water flows past each cross-section of the river. With three piers, the available space for the water to flow through is reduced, leading to higher velocities and more intense recirculation zones. The image provided (Figure 5) illustrates the velocity vectors near the water surface around circular bridge piers. In the double piers configuration (figure 5.a), the velocity vectors showed moderate deviations, with velocities increasing around the piers due to the constriction of the flow path. However, the increase was relatively modest, around 15% above the free stream velocity. In the recirculation zones behind the piers, the velocities were reduced by approximately 20%, indicating the formation of mild vortices and reduced turbulence.

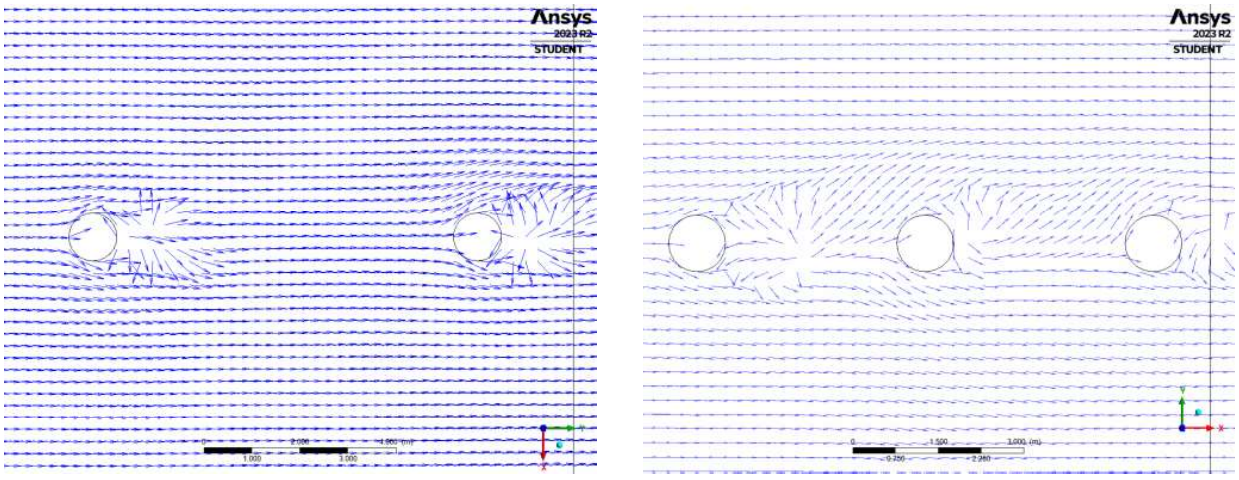

a) Two piers configuration bridge b) Three piers configuration bridge

Fig 5 - X-direction velocity vectors differences between the two piers Two piers configuration bridge (a), and the three piers configuration bridge (b)

In the triple piers configuration (figure 5. b), the velocity vectors revealed more substantial deviations. The flow experienced significant accelerations, with velocities increasing by up to 35% above the free stream velocity around the piers. The recirculation zones were more extensive and pronounced, with velocities reduced by up to 30%, indicating stronger vortex formation and higher turbulence. The presence of an additional pier introduced more complexity and interaction between the recirculation zones, leading to a broader impact on the water flow dynamics.

3.3 Discussion of the wall shear field

For the double piers configuration (figure 6. a), the wall shear field demonstrated moderate shear stress around the piers (between 15 to 21 Pa). The shear stress, τ, is a function of the velocity gradient near the wall, as described by the equation $\tau = \mu (\partial u/\partial y)$, where μ is the fluid dynamic viscosity, u is the velocity, and y is the distance from the wall. The double piers create moderate gradients, leading to manageable levels of shear stress.

In the triple piers configuration, the wall shear field showed increased shear stress, particularly between and downstream of the piers. The higher shear stress can be attributed to the increased velocity gradients caused by the more complex flow patterns and the interactions between the piers. The triple configuration introduces more regions where the flow velocity changes rapidly, leading to higher shear forces acting on the riverbed and the piers themselves. This suggests a more significant impact on sediment transport and potential erosion around the piers, as the increased shear stress can mobilize more sediment particles.

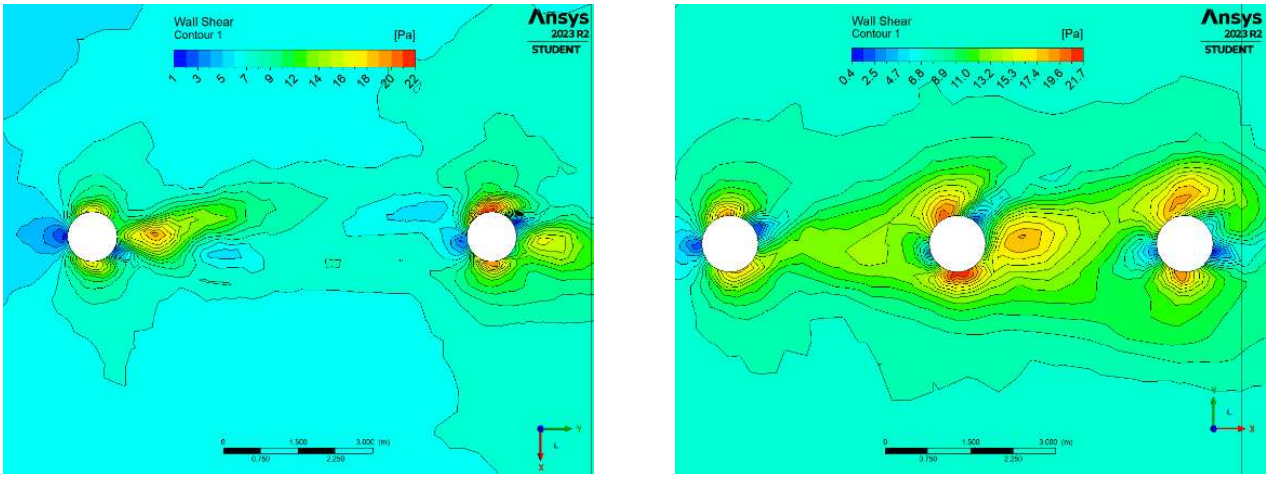

a) Two piers configuration bridge

b) Three piers configuration bridge

Fig. 6 - Shear stress (Pa) at the bottom for the two piers configuration bridge (a), and the three piers configuration bridge (b)

4. CONCLUSIONS

This study highlights the significant influence of bridge pier configurations on water flow patterns, velocity fields, and wall shear stress in river systems. Through detailed numerical simulations, it was found that the triple piers configuration induces more pronounced disturbances and higher shear stress compared to the double piers' setup. These findings align with fluid dynamics principles, as illustrated by the Navier-Stokes and continuity equations.

The addition of a pier in the triple configuration reduces the effective flow area, leading to increased velocities and more intense recirculation zones. This creates larger velocity gradients near the piers, resulting in higher shear stresses. Specifically, in the double piers' configuration, about 30% of the surface exhibits shear stress values above the threshold of 17 Pa, whereas in the triple piers' configuration, this value rises to approximately 50%. This significant increase in the shear stress suggests a higher potential for erosion and sediment transport around the piers.

These findings have crucial implications for bridge design and flood management. The double piers configuration, with its lower impact on water flow and sediment transport, may be preferable in scenarios where minimizing environmental disruption is essential. On the other hand, the triple piers configuration, while potentially offering greater structural stability, requires careful consideration of its environmental impact, particularly regarding increased shear stress and potential erosion.

Future research should focus on experimentally validating these numerical results through laboratory and field studies. Additionally, advanced modeling techniques incorporating real-time data will enhance understanding of the interactions between bridge structures and water flow. By integrating these insights into the design process, innovative solutions that balance the infrastructure need with the environmental sustainability can be developed.

Collaboration among researchers, engineers, and policymakers is essential to advance hydraulic engineering. By working together, safer and more resilient bridge designs that harmonize with natural water dynamics can be developed, effectively mitigating flood risks and minimizing environmental disruption. This study lays the foundation for such collaborative efforts, emphasizing the importance of considering both structural and environmental factors in bridge design.

ACKNOWLEDGEMENT

The authors extend profound gratitude to the dedicated teammates at the INAT and PRISME laboratory.

FUNDING SUPPORT

This research was not funded by any grant

ETHICAL STATEMENT (MUST HAVE)

This study does not contain any studies with human or animal subjects performed by any of the authors.

CONFLICTS OF INTEREST (MUST HAVE)

The authors declare that they have no conflicts of interest to this work.

DATA AVAILABILITY STATEMENT (MUST HAVE)

Data available on request from the corresponding author upon reasonable request.

REFERENCES

[1] Linton, J. (2014). Modern water and its discontents: a history of hydrological renewal. Wiley Interdisciplinary Reviews: Water, 1(1), 111-120. https://doi.org/10.1002/wat2.1009

[2] Charlesworth, S. M., Fontaneda, L. A. S., & Mays, L. W. (2016). Back to the future? History and contemporary application of sustainable drainage techniques. Sustainable Surface Water Management: A Handbook for SuDS, 11-30. https://doi.org/10.1002/9781118897690.ch2

[3] Gleick, P. (1998). The world's water. Issues in Science and Technology, 14(4), 80-88.

[4] Hunter, N.M., Bates, P.D., Neelz, S., Pender, G., Villanueva, I., Wright, N.G. and Mason, D.C. (2008) Benchmarking 2D Hydraulic Models for Urban Flooding. Proceedings of the Institution of Civil Engineers-Water Management, 161, 13-30. https://doi.org/10.1680/wama.2008.161.1.13

[5] Mahjoub, Y., Soualmia, A. and Kourta, A. (2024) Bridge Impact on Water Behavior: Simulation- Application to the Medjerda River in Tunisia. Open Access Library Journal, 11: e11597. https://doi.org/10.4236/oalib.1111597

[6] Zdravkovich, M. M. (1997). Flow around circular cylinders: Volume 2: Applications (Vol. 2). Oxford University Press.

[7] C, Sumer BM, Fuhrman DR, Jacobsen NG, Fredsøe J. 2015 Numerical investigation of flow and scour around a vertical circular cylinder. Phil. Trans. R. Soc. A 373: 20140104. http://dx.doi.org/10.1098/rsta.2014.0104

[8] Jasim, R. A., Hussen, W. Q., Abdullah, M. F., & Zulkifli, R. (2023). Numerical Simulation of Characterization of Hydraulic Jump Over an Obstacle in an Open Channel Flow. Journal of Advanced Research in Fluid Mechanics and Thermal Sciences, 106(1), 1-15. https://doi.org/10.37934/arfmts.106.1.115

[9] Patil, D., Jadhav, R., & Sohoni, P. Analysis of Different Shapes in Bridge Pier Subjected to Extreme Flood Loading. National Conference on Structural Engineering NCRASE – 2020 https://www.researchgate.net/publication/347933498

[10] Nasim, M., Setunge, S., Zhou, S., & Mohseni, H. (2018). An investigation of water-flow pressure distribution on bridge piers under flood loading. Structure and Infrastructure Engineering, 15(2), 219–229. https://doi.org/10.1080/15732479.2018.1545792

[11] Baykal C, Sumer BM, Fuhrman DR, Jacobsen NG, Fredsoe J. 2015 Numerical investigation of flow and scour around a vertical circular cylinder. Phil. Trans. R. Soc. A 373: 20140104. http://dx.doi.org/10.1098/rsta.2014.0104

[12] Aksel, M. (2023) Numerical Analysis of the Flow Structure around Inclined Solid Cylinder and Its Effect on Bed Shear Stress Distribution. Journal of Applied Fluid Mechanics, 16, 1627-1639. https://doi.org/10.47176/jafm.16.08.1697

[13] Roulund, A., Sumer, B.M., Fredsøe, J. and Michelsen, J. (2005). Numerical and Experimental Investigation of Flow and Scour around a Circular Pile. Journal of Fluid Mechanics, 534, 351-401. https://doi.org/10.1017/S0022112005004507

[14] Tartandyo, R.A., Ginting, B.M. and Zulfan, J. (2023) Scale Effects Investigation in Physical Modeling of Recirculating Shallow Flow Using Large Eddy Simulation Technique. Journal of Applied Fluid Mechanics, 17, 43-59. https://doi.org/10.47176/jafm.17.1.1980

[15] Talbi, S. H., Soualmia, A., Cassan, L. and Masbernat, L. (2016) Study of Free Surface Flows in Rectangular Channel over Rough Beds. Journal of Applied Fluid Mechanics, 9, 3023-3031. https://doi.org/10.29252/jafm.09.06.25898